Glutamatergic regulation prevents hippocampal-dependent age-related cognitive decline through dendritic spine clustering

Ana C. Pereira[a,1], Hilary K. Lambert[a], Yael S. Grossman[b,c,d], Dani Dumitriu[b,c,d], Rachel Waldman[b,c], Sophia K. Jannetty[a], Katina Calakos[a], William G. Janssen[b,c], Bruce S. McEwen[a,1], and John H. Morrison[b,c,d,1]

[a]Laboratory of Neuroendocrinology, The Rockefeller University, New York, NY 10065; and [b]Fishberg Department of Neuroscience and Kastor Neurobiology of Aging Laboratories, [c]The Friedman Brain Institute, and [d]Graduate School of Biomedical Sciences, Icahn School of Medicine at Mount Sinai, New York, NY 10029

Contributed by Bruce S. McEwen, November 14, 2014 (sent for review April 8, 2014)

The dementia of Alzheimer's disease (AD) results primarily from degeneration of neurons that furnish glutamatergic corticocortical connections that subserve cognition. Although neuron death is minimal in the absence of AD, age-related cognitive decline does occur in animals as well as humans, and it decreases quality of life for elderly people. Age-related cognitive decline has been linked to synapse loss and/or alterations of synaptic proteins that impair function in regions such as the hippocampus and prefrontal cortex. These synaptic alterations are likely reversible, such that maintenance of synaptic health in the face of aging is a critically important therapeutic goal. Here, we show that riluzole can protect against some of the synaptic alterations in hippocampus that are linked to age-related memory loss in rats. Riluzole increases glutamate uptake through glial transporters and is thought to decrease glutamate spillover to extrasynaptic NMDA receptors while increasing synaptic glutamatergic activity. Treated aged rats were protected against age-related cognitive decline displayed in nontreated aged animals. Memory performance correlated with density of thin spines on apical dendrites in CA1, although not with mushroom spines. Furthermore, riluzole-treated rats had an increase in clustering of thin spines that correlated with memory performance and was specific to the apical, but not the basilar, dendrites of CA1. Clustering of synaptic inputs is thought to allow nonlinear summation of synaptic strength. These findings further elucidate neuroplastic changes in glutamatergic circuits with aging and advance therapeutic development to prevent and treat age-related cognitive decline.

cognitive aging | glutamate | riluzole | neuroplasticity | dendritic spine clustering

Cognitive decline often occurs with aging in rodents (1), nonhuman primates (2), and humans (3). Memory loss (4) and executive impairment (5) are of the most functional importance, mediated primarily by the hippocampus and related areas of the medial temporal lobe and the prefrontal cortex (PFC), respectively. The neural circuits vulnerable to aging are composed of glutamatergic pyramidal neurons that furnish corticocortical connections between the association cortices as well as the excitatory hippocampal connections (2, 6). Dendritic spine changes, which appear to be the primary site of structural plasticity in the adult brain (7), occur in the pyramidal neurons of the PFC (5) and in the hippocampus (8, 9) with aging and correlate with behavioral decline. Spines form the postsynaptic component of most excitatory synapses in the cerebral cortex and are capable of rapid formation, expansion, contraction, and elimination (10, 11).

Synaptic glutamatergic activity is neuroprotective and critical for long-term potentiation (LTP) and memory formation, whereas extrasynaptic NMDA receptor activity promotes long-term depression and excitotoxicity (12, 13). There is some evidence that astrocytic glutamate transporters decrease with aging (14, 15), and consequently reduce glutamate uptake (14, 16, 17). Reduced glutamate uptake can lead to glutamate spillover to the extrasynaptic space with electrophysiological repercussions (14). The potential use of glutamate modulators as a therapeutic target to regulate the synaptic age-related glutamatergic dysregulation in those vulnerable neural circuits remains to be further investigated.

Riluzole is a glutamate modulator that decreases glutamate release (18) and facilitates astrocytic glutamate uptake (19–21). These actions have been suggested to increase glutamate-glutamine cycling, enhancing synaptic glutamatergic activity while preventing excessive glutamate overflow to the extrasynaptic space in rodents (21, 22) and humans (23). Riluzole has also been shown to increase oxidative metabolism with mitochondrial enhancing properties (24) and to increase BDNF expression (25). We hypothesized that improved regulation of the glutamatergic synapse with the glutamate modulator riluzole would promote synaptic NMDA receptor activation while preventing extrasynaptic NMDA activity, thereby protecting against age-related cognitive decline, through induction of neuroplastic changes in the hippocampus and PFC. An important neuroplastic mechanism is clustering of dendritic spines because it significantly empowers neural circuits with nonlinear summation of synaptic inputs (26, 27) and is dependent on neuronal activity (28, 29). For this study, we focused on pyramidal neurons within CA1 and pyramidal neurons in layer 3 of the prelimbic region of medial PFC, an area where we have demonstrated age-related spine loss in middle-aged animals previously (30).

Significance

Aging is often accompanied by cognitive decline. It is of critical importance to understand the synaptic susceptibilities of the glutamatergic neural circuits to age-related cognitive decline and to intervene in this process. Maintenance of synaptic health in the face of aging is a crucially important therapeutic goal. We show that the glutamate modulator, riluzole, prevents age-related memory loss and induces clustering of dendritic spines. Clustering is a critical element of synaptic plasticity that has been previously demonstrated to increase synaptic strength. This study further elucidates neuroplastic changes in the neurocircuits vulnerable to aging and advances therapeutic development to prevent and treat age-related cognitive decline.

Author contributions: A.C.P., D.D., W.G.J., B.S.M., and J.H.M. designed research; A.C.P., H.K.L., Y.S.G., R.W., S.K.J., K.C., and W.G.J. performed research; D.D. contributed new reagents/analytic tools; A.C.P., H.K.L., Y.S.G., W.G.J., B.S.M., and J.H.M. analyzed data; and A.C.P., H.K.L., Y.S.G., B.S.M., and J.H.M. wrote the paper.

The authors declare no conflict of interest.

[1]To whom correspondence may be addressed. Email: apereira@rockefeller.edu, mcewen@mail.rockefeller.edu, or john.morrison@mssm.edu.

This article contains supporting information online at www.pnas.org/lookup/suppl/doi:10.1073/pnas.1421285111/-/DCSupplemental.

Results

Riluzole-Treated Aged Rats Were Protected Against Age-Related Hippocampal Cognitive Decline. We treated 10 Sprague–Dawley rats starting at approximately 10 mo of age with riluzole solution at a dose of 4 mg/kg diluted in water for 17 wk, and another 10 aged-matched animals received regular water. Age-related spine loss occurs by 10 mo of age in medial PFC in the rat (30). Animals were behaviorally tested at baseline and at the end point. Additionally, 10 animals at 3 mo of age were used for behavioral experimentation and served as a young point of comparison. Aged riluzole-treated rats did not show age-related cognitive decline over time in the Y-maze test, a hippocampal-dependent task (31, 32), compared with aged-control rats (Fig. 1). Analysis of covariance using a baseline test as a covariate showed a significant difference between aged-treated and aged-control groups for the percentage of time spent exploring the novel arm (exploration time in novel arm/exploration time in novel + familiar arms) after 9 min [$F(2,17) = 7.32$, $P = 0.0158$*] and 10 min [$F(2,17) = 7.67$, $P = 0.0042$**] into the retention trial at the end point (Fig. 1*A*). To incorporate young-control rats into the analysis, a one-way ANOVA with Tukey multiple comparisons was used to compare the ratios of the three groups at the end point of behavioral testing at 10 min. This analysis showed a significant difference between the three groups [$F(1,18) = 8.86$, $P = 0.0081$**], specifically between aged-control and young-control rats and aged-control and aged-treated rats (Fig. 1*B*). Moreover, the difference in exploration time in the novel and familiar arms showed that aged riluzole-treated rats recognized spatial novelty for a longer duration into the retention trial than aged-control rats, similar to young-control rats (Fig. 1*D*). An ANOVA with repeated measures revealed a significant difference among groups ($F = 14.22$, $P < 0.001$***; main effect) and an interaction between group and time ($P < 0.0001$****). At 9 and 10 min, there was a significant difference between aged-treated and aged-control animals ($P = 0.001$***) and between young-control and aged-control animals ($P < 0.0001$****). Finally, a one-way ANOVA with Tukey multiple comparisons showed a significant difference among groups for total distance moved [$F(2,27) = 6.96$, $P = 0.036$*], indicating, not surprisingly, that mobility decreases with age. There was a reduced mobility in aged-control and aged-treated rats in comparison to young-control rats after 10 min into the retention trial (Fig. 1*C*). However, because there was no significant difference in mobility of aged-control and aged-treated rats, differences in spatial recognition memory ability on the Y-maze were not a result of treatment effects on overall mobility but were more likely a result of learning and memory differences. Riluzole treatment also positively affected other behavioral tests, including object recognition and object placement. The results of an open-field test, a measure of anxiety, were not different among groups. These test results can be found in Figs. S1–S3.

Memory Performance Correlated with the Density of Thin Spines on Apical Dendrites in CA1. Animals were transcardially perfused, and microinjection of Lucifer yellow (LY) in individual neurons for morphometric analysis was performed, with a focus on the pyramidal CA1 neurons in the hippocampus and pyramidal neurons in layer III of prelimbic cortex in medial PFC. The morphometric analysis of LY-filled neurons revealed riluzole treatment-related small reduction of dendritic spines in CA1 (6.9% decrease; $t = 4.02$, $P = 0.0011$**) in comparison to aged untreated animals. A one-way ANOVA comparing the three groups (young, aged-control, and aged-treated) for total spine density in basal dendrites showed a significant difference [$F(2,23) = 8.95$, $P = 0.001$**] (Fig. 2*A*). Tukey post hoc analysis showed a difference between young and aged-treated animals ($P < 0.001$***) and between aged-control and aged-treated animals ($P < 0.05$*). Analysis for mushroom and thin spine

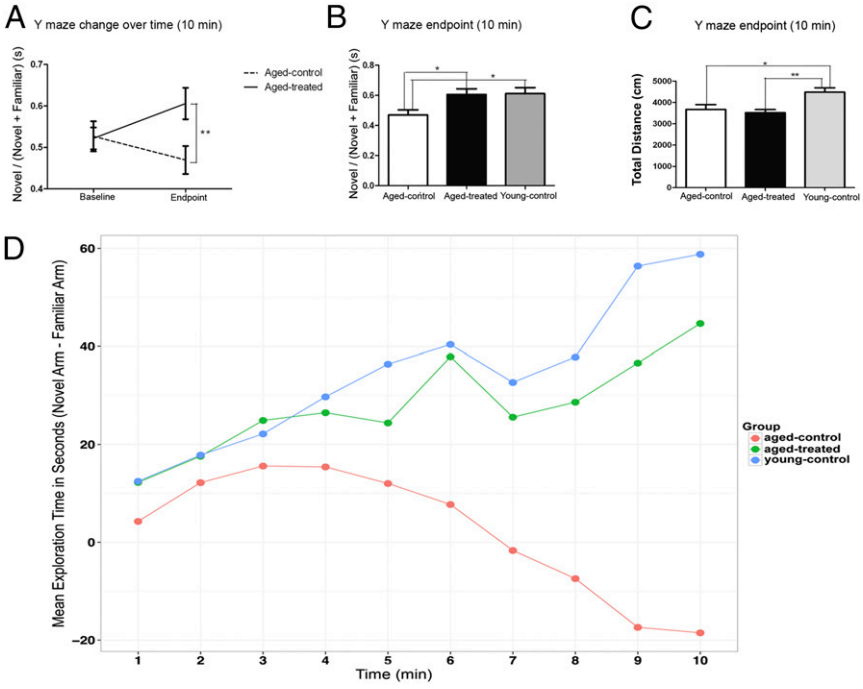

Fig. 1. Riluzole-treated aged rats were protected against age-related hippocampal cognitive decline. Aged-treated animals did not show Y-maze–related cognitive decline in comparison to aged-control animals. (*A*) Change in Y-maze performance from baseline to the end point in aged-treated and aged-control groups ($P = 0.0042$**). (*B*) Performance at the end point of the retention trial at 10 min in aged-control, aged-treated, and young-control groups [$F(1,18) = 8.86$, $P = 0.0081$**]. The aged-treated group is significantly different from aged-control group. (*C*) There was no significant difference in mobility of aged-control and aged-treated rats. (*D*) Difference of exploration time in the novel and familiar arms showed that aged riluzole-treated rats recognized spatial novelty for a longer duration into the retention trial than aged-control rats, in a closer pattern to young-control rats [$F = 14.22$, $P < 0.001$*** (main effect) and $P < 0.0001$**** (interaction between group and time)].

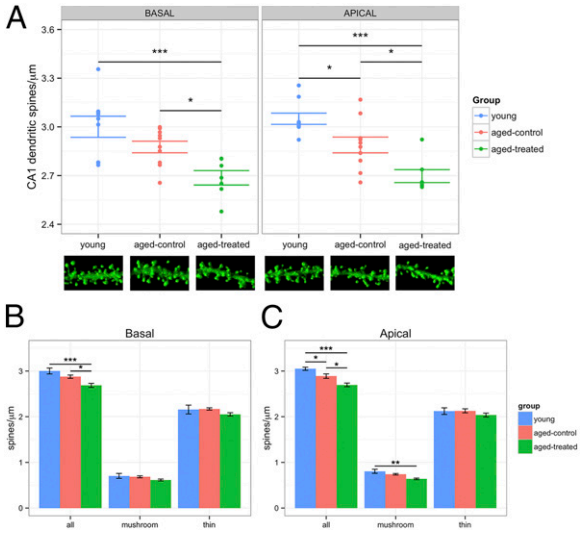

Fig. 2. Morphometric analysis of LY-filled neurons. (*A*) Total spine density was significantly different among groups at basal [$F(2,23) = 8.95$, $P = 0.001$**] and apical [$F(2,23) = 7.22$, $P < 0.001$***] dendrites. (*B*) In basal dendrites, a difference occurred between young and aged-treated animals ($P < 0.001$***) and between aged-control and aged-treated animals ($P < 0.05$*). Mushroom and thin spine subgroups in basal dendrites did not show a significant difference among groups ($P = 0.24$ and $P = 0.39$, respectively). (*C*) In apical dendrites, there was a significant difference between young and aged-control animals ($P < 0.05$*), young and aged-treated animals ($P < 0.001$***), and aged-control and aged-treated animals ($P < 0.05$*). Mushroom spines were different among groups [$F(2,23) = 7.22$, $P = 0.0037$**]. There was a difference between young and aged-treated animals ($P < 0.01$**) but not between young and aged-control animals or aged-control and aged-treated animals. There was no significant difference among groups for thin spine subtype in apical dendrites [$F(2,23) = 0.7$, $P = 0.48$].

subgroups in basal dendrites did not show a significant difference among groups ($P = 0.24$ and $P = 0.39$, respectively) (Fig. 2*B*).

A one-way ANOVA comparing the three groups for total spine density in apical dendrites showed a significant difference [$F(2,23) = 7.22$, $P < 0.001$***] (Fig. 2*A*). Tukey post hoc comparison showed a significant difference between young and aged-control ($P < 0.05$*), young and aged-treated ($P < 0.001$***), and aged-control and aged-treated ($P < 0.05$*) animals. Mushroom spines were different among groups [$F(2,23) = 7.22$, $P = 0.0037$**]. Post hoc Tukey comparison showed a difference between young and aged-treated animals ($P < 0.01$**) but not between young and aged-control animals or aged-control and aged-treated animals (Fig. 2*C*). There was no significant difference among groups for thin spine subtype in apical dendrites [$F(2,23) = 0.7$, $P = 0.48$].

In PFC, there was not a significant change in total spine density between aged riluzole-treated and aged-control animals ($P = 0.52$, $t = 0.65$). Even when the analysis separated the different spine subtypes (thin and mushroom) and dendritic domains (apical and basal), no difference in density was found.

Thin spine density in CA1 in riluzole-treated animals showed a significant positive Pearson correlation with Y-maze performance essentially throughout the trial, including the middle at 5 min ($r = 0.89$, $P = 0.0065$**) and the end at 10 min ($r = 0.81$, $P = 0.026$*). In contrast, density of mushroom spines was unrelated to cognitive performance ($r = -0.23$, $P = 0.60$). Further analysis of thin spine location demonstrated that this correlation with the hippocampal-dependent Y-maze task was driven by apical thin spine density ($r = 0.81$, $P = 0.026$*) (Fig. 3*A*) and not by basal thin spines ($r = -0.26$, $P = 0.57$) (Fig. 3*E*). Apical thin dendritic spine density did not correlate with Y-maze performance in aged-control animals ($r = 0.43$, $P = 0.20$) (Fig. 3*B*). Apical and basal mushroom spine densities were unrelated to behavioral performance in treated animals [$r = -0.62$, $P = 0.13$ (Fig. 3*D*) and $r = 0.28$, $P = 0.5$ (Fig. 3*F*), respectively]. Apical thin spine density also correlated with Y-maze performance in young animals ($r = 0.80$, $P = 0.009$**) (Fig. 3*C*). Errors bars are shown across dendrites and plotted for each animal. In PFC, no correlation was found between behavioral performance and spine density. These results suggest that the riluzole prevention of hippocampal-related cognitive decline during aging is due to neuroplastic changes that occur specifically for thin spines on apical dendrites.

Riluzole-Treated Rats Had an Increase in Clustering of Thin Spines That Correlated with Memory Performance and Was Specific to the Apical Dendrites of CA1. One way by which a small decrease in synaptic density might be related to increased synaptic strength would be if it reflects increased spine clustering. Potentiation at one spine can stabilize and cause retention of that spine, along with its neighbors (33–35). Here, we measured clustering using a Euclidean distance algorithm to calculate the distance of every spine head to its nearest neighboring spine head in 3D space. Because we had observed a small change in spine density between the aged riluzole-treated and untreated animals, we normalized by density to minimize the effect of density on the distances between spine heads. We then used a cumulative distribution plot to observe the distances where there was greater variation between the aged riluzole-treated and the untreated aged animals and tested for significance using a Kolmogorov–Smirnov test with an alpha of 0.05.

To test whether the effect of riluzole elicits a spine distribution similar to what would be observed in young animals, we compared the clustering data from young, aged-control, and aged riluzole-treated animals. We found no significant difference in minimum distances between spine heads between aged-control animals and young-control animals in either the basal or apical

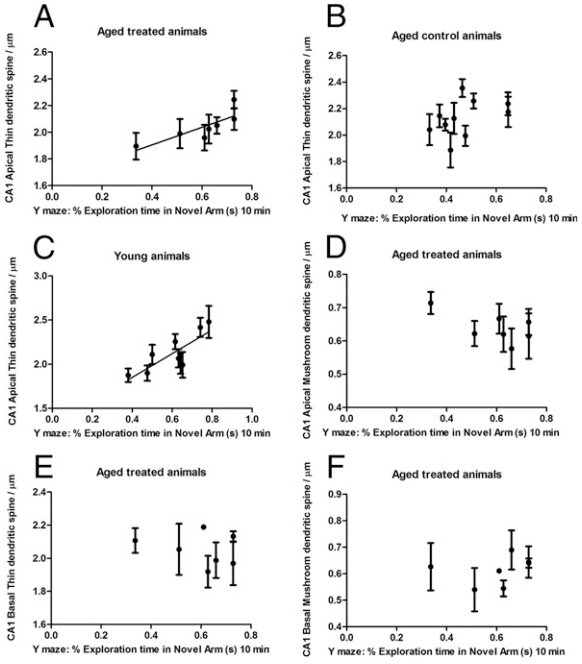

Fig. 3. Memory performance correlated with the density of thin spines on apical dendrites in CA1. Apical thin spine density in CA1 showed a significant positive Pearson correlation with Y-maze performance in aged-treated animals (*A*; $r = 0.81$, $P = 0.026$*) and in young animals (*C*; $r = 0.80$, $P = 0.009$**). (*B*) Apical thin dendritic spine density did not correlate with Y-maze performance in aged-control animals ($r = 0.43$, $P = 0.20$). (*D*) Apical mushroom spines were unrelated to Y-maze performance in treated animals ($r = -0.62$, $P = 0.13$). Basal thin and mushroom densities did not correlate with behavioral performance [$r = -0.26$, $P = 0.57$ (*E*) and $r = 0.28$, $P = 0.5$ (*F*), respectively].

dendrites of CA1. Between young animals and riluzole-treated animals, however, there was a significant difference in spine clustering of both thin ($P = 0.005$**) and mushroom ($P = 0.012$**) spines in apical dendrites, although not in basal dendrites. Analysis of the cumulative distribution plot demonstrated that this difference was due to a higher occurrence of small distances in riluzole-treated animals compared with young and aged-control animals, indicating that the increased spine clustering observed in riluzole-treated aged animals is somewhat different from the spine distribution observed in young animals.

We found a significant difference in nearest neighbor distance between riluzole aged-treated and aged untreated animals in thin spines ($P = 0.0026$**) but not in mushroom spines ($P = 0.4181$) in area CA1 of the hippocampus. From analysis of the cumulative distribution plot, we saw that this distance was due to a significant increase of the frequency of small distances between spine heads (i.e., increased clustering). To isolate the effects of this difference in distance between spine heads better, we separated the dendrites into apical and basal categories. We found that the difference in distances between spine heads was primarily driven by the apical thin spines ($P = 0.0051$**) (Fig. 4 *A* and *B*), but not the basal thin spines ($P = 0.069$). Neither the apical nor the basal mushroom spines exhibited any significant differences in distance between spine heads in riluzole-treated and untreated animals. Fig. 5 shows a schematic representation of increased clustering of thin spines in apical dendrites in aged-treated animals in comparison to aged-control and young animals. Because it has been well established that permanent spines may enhance stabilization of neighboring spines (36), and because mushroom spines tend to be more permanent than thin spines (37), we specifically tested the clustering of each thin spine to its nearest mushroom neighbor. We found no significant difference between thin-mushroom clustering of riluzole-treated and aged-control animals at any distance in the CA1 neurons, thus indicating that the clustering we observe is due to thin–thin interactions rather than thin–mushroom interactions. No significant difference was found between riluzole-treated and untreated animals in layer III of the PFC. Dendritic arborization analysis also did not show significant differences in dendritic length between aged-treated and aged-control groups in CA1 or PFC.

To test whether spine clustering was correlated to performance, the data from the cumulative distributions were normally fitted by animal. We analyzed the area under the curve between the normalized distances of 0.6 and 0.9 because this area was where the strongest effect of riluzole was observed between drug-treated and control animals. For normally distributed data, the area under the curve can either be calculated as a z-score or converted to a cumulative probability, which demonstrates the possibility of any data point chosen randomly originating from that area. Using cumulative probability, we found that there was a significant correlation between the cumulative probability and the performance in the Y-maze at 5 min ($r = 0.72$, $P = 0.042$*) in treated animals (Fig. 4*C*).

Discussion

We present here a potential treatment for age-related cognitive decline targeting aging glutamatergic circuits along with complex neuroplastic mechanisms that permits, at least partially, retention of memory performance dependent on hippocampus and vulnerable to aging. Dendritic spine clustering appears to be the core neuroplastic mechanism that prevented hippocampal-dependent age-related cognitive decline with this glutamate modulator treatment. Electrophysiological studies and computational modeling have shown that clustering of dendritic spines significantly empowers neural circuits with nonlinear summation of synaptic inputs (27, 38). Specifically, nearby thin dendrites of pyramidal neurons on the same branch sum sigmoidally, whereas widely separated inputs or inputs to different branches sum linearly (26). Clustering of synaptic inputs has also been shown to be dependent on neuronal activity (28, 29) and is induced by LTP (35). Furthermore, in hippocampal pyramidal neurons, LTP at individual synapses lowers the threshold for potentiation at neighboring synapses within ∼10 μm on the same dendritic branch (34). The treatment-induced spine clustering in CA1 involved thin spines but not mushroom spines, and it was specific to apical dendrites. Further analysis showed increased thin–thin rather than mushroom–thin interactions when comparing aged-treated and aged-control animals. Interestingly, aged-treated animals presented a higher occurrence of clustering than young animals, thus showing a change in clustering distribution with aging under a partially compensated state. Notably, the dendritic domains analyzed in CA1 were in the stratum radiatum, which receives inputs from Schaffer collaterals (39). Importantly, thin spines represent the most adaptive subtype of spine, capable of experience-dependent rewiring of neuronal circuits (37). Clustering of the spines with thin–thin interaction may represent a compensatory mechanism generating more efficient glutamatergic transmission. Other neuroplastic mechanisms may also be induced by riluzole, including alterations in mushroom spines that could be contributing to the clustering environment, although the dominant role of the thin spines that emerged lends further support to the importance of this spine class with respect to aging, plasticity, and cognitive performance (2).

Our clustering results also reinforce previous studies finding that the glutamate modulator riluzole likely increases synaptic glutamatergic activity (22, 23). The key mechanism of action of riluzole to prevent aging may well be the increase of glutamate uptake by glia transporters (19–21), correcting their decreased function that occurs with aging (14, 16, 17). Previous work has shown age-related partial rescue of a hippocampal glutamate transporter expression and spatial memory with riluzole treatment (15). By maintaining tighter control of glutamate levels at the synapse and rapid cycling of glutamate-glutamine (22), synaptic glutamatergic activity may be increased while preventing glutamate overflow and activation of extrasynaptic NMDA receptors. Other mechanisms induced by riluzole could also be involved in the prevention of age-related cognitive decline, including increased BDNF expression (25) and oxidative metabolism

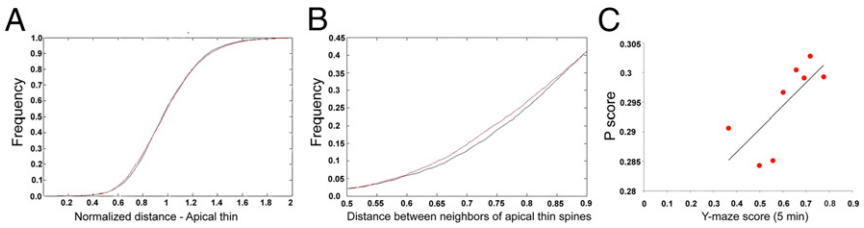

Fig. 4. Cumulative distributions of normalized distances between spine heads. Riluzole-treated rats had an increase in clustering of thin spines that correlated with memory performance and was specific to the apical dendrites of CA1. Red indicates riluzole-treated rats and black indicates control rats. (*A*) Cumulative distribution of apical thin spines. Riluzole-treated animals have a significant shift toward a higher frequency of small distances between spine heads than control animals ($P = 0.0051$**). (*B*) Enlarged image of *A*, which allows for better observation of the higher frequency of small distances in drug-treated animals. (*C*) There is a significant correlation between apical thin spine clustering and performance on the Y-maze ($P = 0.042$*).

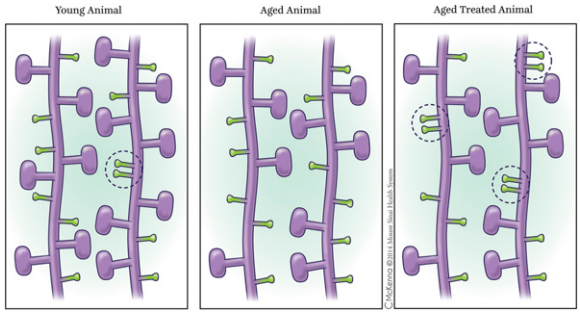

Fig. 5. Schematic representation of apical dendrites with spine clustering in CA1. Aged-treated animals presented with increased thin–thin interaction dendritic spine clustering (*Right*) in comparison to aged-control animals (*Center*) and young animals (*Left*), as shown in the encircled areas. Dendritic spine clustering has been shown to empower neural circuits with nonlinear summation of synaptic inputs. In relation to spine density, there is slightly diminished mushroom density in aged-treated animals in comparison to young animals (represented in the figure) but there is no significant thin or mushroom spine density difference between aged-control and aged-treated animals (main text). Although connectivity is altered and thin spine clustering is increased in treated animals, total thin spine density in apical dendrites is not significantly changed when comparing the three groups, as represented in the schematic figure.

(24). Future experiments could individually block each of these pathways (i.e., hippocampal infusion of glutamate transport inhibitors, use of BDNF antibody) to investigate which one(s) block the effect on behavior, further pinpointing the critical pathways.

Synaptic networks adapt to the environment through a continuous turnover process (7). Neuroplastic changes associated with learning and memory have been shown in association with formation of new spines, and pruning with elimination of spines also appears to be critical (35, 40–44). Notably, LTP on mature hippocampal neurons shows that synapse loss is perfectly counterbalanced by enlargement of the remaining excitatory synapses (45). In some cases, the increase in spine formation and elimination is similar, resulting in no marked change in spine density (46–48). As in this study, apical thin spines did not show a significant change in dendritic spine density, although there is a positive correlation between behavior and spine density and clustering. The results presented here not only mechanistically demonstrate the structural modifications associated with the behavioral enhancement produced by riluzole but also expand on the diversity and complexity of plasticity mechanisms with therapeutic relevance. It will also be interesting to investigate, when new agents are discovered to prevent cognitive decline, if clustering is a common neuroplastic compensatory mechanism in the aging brain.

In conclusion, our data suggest that riluzole may have the potential to treat or even prevent age-associated memory decline and that these findings in aged rodents can be translated to study the impact of riluzole on cognitive function in the aging human brain. This study also suggests that further exploration of novel glutamate modulators that target circuits vulnerable to aging represents a promising therapeutic strategy.

Methods

Animals. Aged, male Sprague–Dawley rats (n = 20, retired breeders; Harlan Laboratories) were housed at The Rockefeller University from 9 until 14–15 mo of age. Young, male Sprague–Dawley rats (n = 10) ordered from the same source were housed in the same facility from 3 until 4–5 mo of age. All rats were pair-housed in controlled conditions (30–50% humidity, 21 ± 2 °C, 12-h light/dark cycle). All procedures were done in agreement with the National Institutes of Health and The Rockefeller University Institutional Animal Care and Use Committee guidelines.

Treatment. Aged-treated rats (n = 10) had ad libitum access to riluzole solution, and aged-control (n = 10) and young-control (n = 10) rats had ad libitum access to tap water. Aged animals received riluzole or water for 17 wk. All rats had ad libitum access to food. The riluzole compound (Sigma–Aldrich, Inc.) was dissolved in tap water at a concentration of 110 μg/mL, translating to ~4.0 $mg \cdot kg^{-1} \cdot d^{-1}$ p.o., a dose previously tested in rats (21). To make the solution, riluzole was stirred in room temperature tap water overnight. All containers with riluzole were covered in tin foil to prevent light exposure. Fresh solutions were made every 2–3 d for the duration of treatment.

Y-Maze. The Y-maze task (31, 32) was used to measure spatial recognition memory at baseline and end point (17 wk). The task consisted of a 15-min acquisition trial, a 4-h intertrial delay, and a 10-min retention trial. During the acquisition trial, rats were placed facing away from the center of the maze in one arm (start arm) and were allowed to explore two arms (start arm and familiar arm). The third arm (novel arm) was blocked off with a Plexiglas panel identical to the other walls of the Y-maze. During the retention trial, rats were placed in the same orientation in the start arm and allowed to explore all three arms. Start, familiar, and novel arms were rotated between rats. Three different spatial cues were placed 1 foot above each arm of the maze on the curtain surrounding the apparatus (Fig. S4*A*). Used corncob bedding from each rat being tested was mixed and spread over the floor of the maze to reduce anxiety. Each arm of the maze was 14.5 × 48.26 cm. To ensure commitment to entering an arm, rat movement was recorded in a more conservative zone of 14.5 × 45 cm in each arm. If spatial recognition memory is intact, rats should explore the novel arm more than the familiar arm during the retention trial, given their natural tendency to explore novel environments. Extent of exploration was assessed in terms of time(s) spent in arms, number of entries into arms, latency(s) to enter arms for the first time, and arm entered first. See Table S1 and *SI Methods* for further methods on behavior.

Confocal Laser Scanning Microscopy and NeuronStudio Spine Morphological Analysis. Spine imaging and analysis were conducted according to Bloss et al. (30). Concentric circles in increments of 50 μm were drawn over the 25-fold trace of the neuron from the center of the soma to provide a systematic sampling of proximal (100 μm), intermediate (150 μm), and distal (200 μm) dendritic segments. A random subset of six to eight neurons was imaged for each animal. When possible, two segments at each distance from the soma in the apical tree per neuron and two segments at each distance from the soma in the basal tree per neuron (~8–12 segments) were imaged using a Zeiss 510 confocal microscope equipped with an argon laser, Zeiss oil-immersion objective (magnification of 40× and N.A. of 1.4), and ZEN software for laser scanning microscopy (49). Segments from dendritic branches had to satisfy the following criteria: (*i*) located within a depth of 100 μm from the surface of the section because of the limited working distance of the objective, (*ii*) parallel to or at acute angles relative to the coronal surface of the section to allow for unambiguous identification of spines, (*iii*) segments had no overlap with other branches that would obscure visualization of spines, (*iv*) dendrites had to be terminating rather than bifurcating, and (*v*) dendrite image had to be captured at least 10 μm from both the origin and the tip.

Conditions such as laser excitation (458 nm), florescence emission capture (505–530 nm), pinhole size (1 Airy unit), speed (3.2 μs per pixel), and frame average (two frames per z-step) were held constant throughout. Confocal z-stacks were taken using a Zeiss objective (magnification of 40× and N.A. of 1.4) with a digital zoom of 4.0, a z-step size of 0.1 μm, and a pixel resolution of 512 × 512, yielding an image with pixel dimensions of 0.05 × 0.05 × 0.1 μm. Z-stacks were deconvoluted using AutoDeblur software to improve voxel resolution and reduce optical aberration along the *z* axis. Images were then imported and analyzed using custom-built NeuronStudio software (50). Analysis on Neuronstudio was performed in a semiautomated manner. In short, the settings for the automated analysis were 10% threshold correction, 350 voxels for minimum stubby size, five voxels for minimum nonstubby size, 0.8 neck ratio, 2:1 thin ratio, and 0.35 for mushroom size, with review and correction by the user in regard to spine location, subtype, and existence.

Dendritic Spine Clustering Analysis. Spine clustering was calculated utilizing a Euclidean distance algorithm in three dimensions using MATLAB 2010a (MathWorks). In brief, the distance between each spine head and its nearest neighboring spine head was collected and then normalized by the density of spines per dendrite. The distances were plotted as a cumulative distribution, and significance was tested using the Kolmogorov–Smirnov test, a

nonparametric test for similarity between continuous, 1D probability distributions. These tests were performed on all the dendrites of the PFC and CA1, as well as on divisions within each region of spine subtype (apical and basal). The Euclidean distance was defined as follows:

$$d\,(p,q) = d(q,p) = \sqrt{(q_1 - p_1)^2 + (q_2 - p_2)^2 + \ldots + (q_n - p_n)^2} = \sqrt{\sum_{i=1}^{n} (q_1 - p_1)^2}.$$

To test correlation of behavior with spine clustering individually, each set of spine head distances was fit to a normal distribution by animal. A cutoff was chosen between 0.6 and 0.9 based on the distances that had been found to be significantly different between the drug-treated and control animals. The area within this range was calculated by standardizing the normal distribution and converting the z-score obtained from the standardization to a cumulative probability score. The cumulative probability score allows for analysis of the likelihood of randomly choosing a spine with a normalized distance between 0.6 and 0.9. This value was then correlated to the animals' performance in the Y-maze.

ACKNOWLEDGMENTS. We thank Dr. Howard Fillit for mentorship guidance to A.C.P., Dr. Richard Hunter for study design assistance, Dr. Joel Correa da Rosa for statistical analysis assistance, and Kaitlyn Hajdarovic for computer assistance. This work was supported by the Dana Foundation, Alzheimer's Drug Discovery Foundation, and Stavros Niarchos Foundation, and partially supported by Grant 8 UL1 TR000043 from the National Center for Research Resources and the National Center for Advancing Translational Sciences and by Grant R37 AG06647 from the National Institute on Aging (NIH).

1. Burke SN, Barnes CA (2006) Neural plasticity in the ageing brain. *Nat Rev Neurosci* 7(1):30–40.
2. Morrison JH, Baxter MG (2012) The ageing cortical synapse: Hallmarks and implications for cognitive decline. *Nat Rev Neurosci* 13(4):240–250.
3. Buckner RL (2004) Memory and executive function in aging and AD: Multiple factors that cause decline and reserve factors that compensate. *Neuron* 44(1):195–208.
4. Barnes CA (1979) Memory deficits associated with senescence: A neurophysiological and behavioral study in the rat. *J Comp Physiol Psychol* 93(1):74–104.
5. Dumitriu D, et al. (2010) Selective changes in thin spine density and morphology in monkey prefrontal cortex correlate with aging-related cognitive impairment. *J Neurosci* 30(22):7507–7515.
6. Morrison JH, Hof PR (1997) Life and death of neurons in the aging brain. *Science* 278(5337):412–419.
7. Holtmaat A, Svoboda K (2009) Experience-dependent structural synaptic plasticity in the mammalian brain. *Nat Rev Neurosci* 10(9):647–658.
8. von Bohlen und Halbach O, Zacher C, Gass P, Unsicker K (2006) Age-related alterations in hippocampal spines and deficiencies in spatial memory in mice. *J Neurosci Res* 83(4): 525–531.
9. deToledo-Morrell L, Geinisman Y, Morrell F (1988) Age-dependent alterations in hippocampal synaptic plasticity: Relation to memory disorders. *Neurobiol Aging* 9(5-6): 581–590.
10. Grutzendler J, Kasthuri N, Gan WB (2002) Long-term dendritic spine stability in the adult cortex. *Nature* 420(6917):812–816.
11. Trachtenberg JT, et al. (2002) Long-term in vivo imaging of experience-dependent synaptic plasticity in adult cortex. *Nature* 420(6917):788–794.
12. Hardingham GE (2006) Pro-survival signalling from the NMDA receptor. *Biochem Soc Trans* 34(Pt 5):936–938.
13. Hardingham GE, Bading H (2010) Synaptic versus extrasynaptic NMDA receptor signalling: Implications for neurodegenerative disorders. *Nat Rev Neurosci* 11(10): 682–696.
14. Potier B, et al. (2010) Reduction in glutamate uptake is associated with extrasynaptic NMDA and metabotropic glutamate receptor activation at the hippocampal CA1 synapse of aged rats. *Aging Cell* 9(5):722–735.
15. Brothers HM, et al. (2013) Riluzole partially rescues age-associated, but not LPS-induced, loss of glutamate transporters and spatial memory. *J Neuroimmune Pharmacol* 8(5):1098–1105.
16. Wheeler DD, Ondo JG (1986) Time course of the aging of the high affinity L-glutamate transporter in rat cortical synaptosomes. *Exp Gerontol* 21(3):159–168.
17. Vatassery GT, Lai JC, Smith WE, Quach HT (1998) Aging is associated with a decrease in synaptosomal glutamate uptake and an increase in the susceptibility of synaptosomal vitamin E to oxidative stress. *Neurochem Res* 23(2):121–125.
18. Martin D, Thompson MA, Nadler JV (1993) The neuroprotective agent riluzole inhibits release of glutamate and aspartate from slices of hippocampal area CA1. *Eur J Pharmacol* 250(3):473–476.
19. Fumagalli E, Funicello M, Rauen T, Gobbi M, Mennini T (2008) Riluzole enhances the activity of glutamate transporters GLAST, GLT1 and EAAC1. *Eur J Pharmacol* 578(2-3): 171–176.
20. Frizzo ME, Dall'Onder LP, Dalcin KB, Souza DO (2004) Riluzole enhances glutamate uptake in rat astrocyte cultures. *Cell Mol Neurobiol* 24(1):123–128.
21. Banasr M, et al. (2010) Glial pathology in an animal model of depression: reversal of stress-induced cellular, metabolic and behavioral deficits by the glutamate-modulating drug riluzole. *Mol Psychiatry* 15(5):501–511.
22. Chowdhury GM, et al. (2008) Chronic riluzole treatment increases glucose metabolism in rat prefrontal cortex and hippocampus. *J Cereb Blood Flow Metab* 28(12): 1892–1897.
23. Brennan BP, et al. (2010) Rapid enhancement of glutamatergic neurotransmission in bipolar depression following treatment with riluzole. *Neuropsychopharmacology* 35(3):834–846.
24. Mu X, Azbill RD, Springer JE (2000) Riluzole improves measures of oxidative stress following traumatic spinal cord injury. *Brain Res* 870(1-2):66–72.
25. Mizuta I, et al. (2001) Riluzole stimulates nerve growth factor, brain-derived neurotrophic factor and glial cell line-derived neurotrophic factor synthesis in cultured mouse astrocytes. *Neurosci Lett* 310(2-3):117–120.
26. Polsky A, Mel BW, Schiller J (2004) Computational subunits in thin dendrites of pyramidal cells. *Nat Neurosci* 7(6):621–627.
27. Larkum ME, Nevian T (2008) Synaptic clustering by dendritic signalling mechanisms. *Curr Opin Neurobiol* 18(3):321–331.
28. Kleindienst T, Winnubst J, Roth-Alpermann C, Bonhoeffer T, Lohmann C (2011) Activity-dependent clustering of functional synaptic inputs on developing hippocampal dendrites. *Neuron* 72(6):1012–1024.
29. Kavalali ET, Klingauf J, Tsien RW (1999) Activity-dependent regulation of synaptic clustering in a hippocampal culture system. *Proc Natl Acad Sci USA* 96(22): 12893–12900.
30. Bloss EB, et al. (2011) Evidence for reduced experience-dependent dendritic spine plasticity in the aging prefrontal cortex. *J Neurosci* 31(21):7831–7839.
31. Dellu F, Mayo W, Cherkaoui J, Le Moal M, Simon H (1992) A two-trial memory task with automated recording: Study in young and aged rats. *Brain Res* 588(1):132–139.
32. Conrad CD, Galea LA, Kuroda Y, McEwen BS (1996) Chronic stress impairs rat spatial memory on the Y maze, and this effect is blocked by tianeptine pretreatment. *Behav Neurosci* 110(6):1321–1334.
33. Poirazi P, Mel BW (2001) Impact of active dendrites and structural plasticity on the memory capacity of neural tissue. *Neuron* 29(3):779–796.
34. Harvey CD, Svoboda K (2007) Locally dynamic synaptic learning rules in pyramidal neuron dendrites. *Nature* 450(7173):1195–1200.
35. De Roo M, Klauser P, Muller D (2008) LTP promotes a selective long-term stabilization and clustering of dendritic spines. *PLoS Biol* 6(9):e219.
36. Liao D, Hessler NA, Malinow R (1995) Activation of postsynaptically silent synapses during pairing-induced LTP in CA1 region of hippocampal slice. *Nature* 375(6530): 400–404.
37. Kasai H, Matsuzaki M, Noguchi J, Yasumatsu N, Nakahara H (2003) Structure-stability-function relationships of dendritic spines. *Trends Neurosci* 26(7):360–368.
38. Govindarajan A, Kelleher RJ, Tonegawa S (2006) A clustered plasticity model of long-term memory engrams. *Nat Rev Neurosci* 7(7):575–583.
39. Blackstad TW (1956) Commissural connections of the hippocampal region in the rat, with special reference to their mode of termination. *J Comp Neurol* 105(3):417–537.
40. Segal M (2005) Dendritic spines and long-term plasticity. *Nat Rev Neurosci* 6(4): 277–284.
41. Goldin M, Segal M, Avignone E (2001) Functional plasticity triggers formation and pruning of dendritic spines in cultured hippocampal networks. *J Neurosci* 21(1): 186–193.
42. Bourne J, Harris KM (2007) Do thin spines learn to be mushroom spines that remember? *Curr Opin Neurobiol* 17(3):381–386.
43. Holtmaat A, Wilbrecht L, Knott GW, Welker E, Svoboda K (2006) Experience-dependent and cell-type-specific spine growth in the neocortex. *Nature* 441(7096): 979–983.
44. Engert F, Bonhoeffer T (1999) Dendritic spine changes associated with hippocampal long-term synaptic plasticity. *Nature* 399(6731):66–70.
45. Bourne JN, Harris KM (2011) Coordination of size and number of excitatory and inhibitory synapses results in a balanced structural plasticity along mature hippocampal CA1 dendrites during LTP. *Hippocampus* 21(4):354–373.
46. Xu T, et al. (2009) Rapid formation and selective stabilization of synapses for enduring motor memories. *Nature* 462(7275):915–919.
47. Yang G, Pan F, Gan WB (2009) Stably maintained dendritic spines are associated with lifelong memories. *Nature* 462(7275):920–924.
48. Caroni P, Donato F, Muller D (2012) Structural plasticity upon learning: Regulation and functions. *Nat Rev Neurosci* 13(7):478–490.
49. Rodriguez A, Ehlenberger DB, Hof PR, Wearne SL (2006) Rayburst sampling, an algorithm for automated three-dimensional shape analysis from laser scanning microscopy images. *Nat Protoc* 1(4):2152–2161.
50. Wearne SL, et al. (2005) New techniques for imaging, digitization and analysis of three-dimensional neural morphology on multiple scales. *Neuroscience* 136(3): 661–680.